Preparation of Asymmetric PEEKWC Flat Membranes with Different Microstructures by Wet Phase Inversion

M. G. Buonomenna, A. Figoli, J. C. Jansen, E. Drioli

Institute of Membrane Technology, ITM-CNR, c/o University of Calabria, Via P. Bucci, Cubo 17/c, 87030 Rende (CS), Italy

Received 21 July 2003; accepted 12 November 2003

ABSTRACT: Membranes with controlled morphology were prepared by wet phase inversion from PEEKWC, a modified polyetheretherketone. Different membrane structures were obtained by using different nonsolvent/solvent pairs. The influence of several parameters, such as the composition of the polymer solution (concentration, type of solvent), the composition of the coagulation bath, and the exposure time before immersion in the coagulation bath, on the membrane morphology was studied. The PEEKWC/solvent/nonsolvent phase diagrams, with various solvent/nonsolvent combinations, were determined and correlated to the process of phase separation during membrane formation. Using solvent/nonsolvent pairs with a high mutual affinity (DMF/water, DMA/water), porous membranes for possible application in microfiltration were obtained. The THF/water combination allowed the formation of asymmetric membranes with a dense skin layer, suitable for gas separation applications. Nitrogen permeance of all porous membranes was measured as function of pressure. Application of the Dusty Gas model permitted a qualitative description of the pore size and membrane morphology in relation to the membrane preparation conditions.© 2004 Wiley Periodicals, Inc. J Appl Polym Sci 92: 576—591, 2004

Key words: membrane formation; phase inversion; phase diagrams; polyetheretherketone (PEEKWC); gas permeation

INTRODUCTION

PEEKWC is a modified polyetheretherketone having a lactone group attached to the backbone (Scheme 1).[1,2] One of its major advantages is that it preserves the good thermal and mechanical properties of the traditional PEEK but, compared to the latter, it has a much higher solubility, also found in common organic solvents such as chloroform and tetrahydrofuran (THF). Therefore, it is well suited for preparation of polymeric membranes by phase inversion techniques. Several studies have been presented on the use of PEEKWC as a membrane-forming material[3–5] under different conditions.

Only recently a systematic study on the morphology of the asymmetric membranes by phase inversion as a function of the solvent and polymer concentration has been presented for flat membranes[6] and for hollow fiber membranes[7]. In the present article, a wider range of conditions, such as solvent/nonsolvent combination, coagulation bath composition, and time interval between casting and coagulation, have been explored.

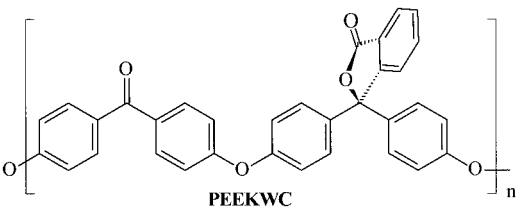

PEEKWC

Scheme 1 Structure of PEEKWC.

Nonsolvent induced phase separation (NIPS)

NIPS is the most common phase inversion method used for membrane preparation. This technique has been described extensively in the literature for a large number of polymer/solvent/nonsolvent combinations.[8–20] Upon immersion of the casting solution into a coagulation bath, diffusion of a solvent and a nonsolvent across the interface between polymer solution and nonsolvent induces phase inversion of the polymer solution. Subsequently, solidification of the polymer-rich phase, e.g., by gelation, crystallization, or vitrification, yields the final membrane. The actual process of phase inversion depends on a number of thermodynamic and kinetic factors, which determine the membrane morphology. Of fundamental importance is the exchange rate of solvent and nonsolvent in the cast polymeric solution.[11] Depending on these exchange rates, membranes with symmetric or asymmetric structures are formed. Based on the calculated composition paths and supported by experimental

Correspondence to: M. G. Buonomenna (mg.buonomenna@itm.cnr.it).

Journal of Applied Polymer Science, Vol. 92, 576—591 (2004)

TABLE I
Properties of Some Good Solvents for PEEKWC

Solvent	Volatility	δ^a $cal^{1/2}$ $cm^{-3/2}$	Miscibility with polar solvents	Miscibility with nonpolar solvents
N-Methylpyrrolidone	——	11.3 m	++	—
Dimethylsulfoxide	——	12.0 m	+++	—
N,N-Dimethylacetamide	——	10.8 m	++	—
N,N-Dimethylformamide	——	12.1 m	+++	—
Tetrahydrofuran	++	9.1 m	+	++
Chloroform	++	9.3 p	+—	+++
Dichloromethane	+++	9.7 p	+—	+++

[a] Hildebrand solubility parameter.[23] Letter indicates capacity to form hydrogen bonds (m, medium hydrogen bonding capacity; p, poor hydrogen bonding capacity.

data, Reuvers et al.[21,22] classified membrane formation processes into two groups: instantaneous demixing systems and systems that show delayed onset of demixing. Membranes formed by a delayed demixing mechanism show a porous (often closed-cell, macrovoid free) substructure with a dense relatively thick skin layer while membranes formed by instantaneous demixing generally show a highly porous substructure (with macrovoids) and a finely porous skin layer. Which specific process dominates is mainly determined by the solvent/nonsolvent affinity and the solvent concentration in the coagulation bath. In particular, in the case of good solvent/nonsolvent miscibility,[23] the latter can easily penetrate into the casting solution and create a porous structure. In this light, the good solubility of PEEKWC in solvents having different polarities and miscibilities with nonsolvents (Table I) thus allows one to obtain various membrane morphologies.

The objectives of this work are as follows:

- Exploration of the influence of the main experimental variables (polymer concentration, coagulation bath composition, type of solvent and nonsolvent, exposure time of the cast film to the air before coagulation) on the membrane morphology and transport properties.
- Correlation of the morphology to the demixing process in terms of kinetic and thermodynamic parameters.

The final aim is to establish which conditions are required to produce membranes for different separation processes, such as microfiltration, ultrafiltration, and gas separation/pervaporation.

Characterization of porous membranes by gas permeation

Although porous membranes generally are not used for gas separation, gas permeability measurements are frequently used to characterize them. Carried out under standard conditions, gas permeation measurements offer a simple and rapid quality test of membranes or their porous supports. For example, the Gurly number (i.e., the time required for 10 mL of air to permeate through 1 square inch of membrane at a pressure of 12.2 in. of water) is used as a measure of the "quality" of microporous membranes.[24] Also, in the case of composite asymmetric membranes with an ultrathin highly permeable dense skin layer, characterization of the gas permeability of the support layer is important, as the porous support layer may contribute significantly to the total resistance of the membrane.[25]

Information that can be obtained from gas permeance measurements of porous membranes is not limited to qualitative or quantitative data on their transport properties. By measurement of the gas permeance at different feed pressures, one can obtain information on the membrane morphology, in particular on the average pore size.[25–29]

Quantitative description of gas flow in porous media

Gas permeability of porous media is pressure dependent and, if surface transport phenomena can be neglected, this pressure dependence can be described with relatively simple expressions. For homogeneous porous media, such as symmetric microporous membranes, the pressure dependence of the permeance (P/L) can be described using the Dusty Gas Model, in simplified form:[28]

$$P/L = A + B \times p_{mean}, \tag{1}$$

in which P is the permeability coefficient, L is the membrane thickness, and p_{mean} is the mean pressure across the membrane, given by:

$$p_{mean} = (p_{feed} + p_{permeate}) / 2 \tag{2}$$

Parameters A and B depend on the membrane morphology (porosity, pore size, and tortuosity) and can be obtained by a linear regression of the experimental

TABLE II
Summary of the Membrane Preparation Conditions[a]

Solvent used	DMA			DMF			THF		
Polymer concentration (wt %)	10	15	19	10	15	19	10	15	19
Coagulation bath composition (% v/v)									
Coagulant: water	100 water	0% DMA 40% DMA 60% DMA	100 water	100 water	100 water	100 water	100 water	100 water	100 water
Coagulant: isopropanol					0% DMF 25% DMF 50% DMF				
Exposure time before immersion in coagulation bath									
Coagulant: water	45 s	0 s 45 s 4 min complete evaporation	0 s 45 s	45 s	0 s 45 s 4 min complete evaporation	0 s 45 s	20 s	20 s	20 s

[a] Casting thickness 250 μm; coagulation bath temperature 25°C except for the membranes from the system PEEKWC/DMF/water. In fact, membranes 10 wt % are prepared by coagulation bath at 15, 25, and 40°C to evaluate the effect of this variable on the system.

permeance data. They represent the contributions of Knudsen flow and viscous flow, respectively, and their ratio (B/A) is directly proportional to the average pore size r_p:

$$r_p = 16\eta\nu / 3 \times B / A \quad (3)$$

Where η is the viscosity of the gas and ν is the mean molecular velocity, given by:

$$\nu\pi = \sqrt{8/RTM} \quad (4)$$

The pressure dependence decreases with decreasing pore size and, in the case of ideal Knudsen flow, the permeance becomes pressure independent.

Measuring the permeance as a function of the mean pressure and then normalizing for the extrapolated permeance at $p_{mean} = 0$ [(i.e., parameter A in eq. (1)] gives the relative permeance:

$$(P / L)_{rel} = 1 + (B / A) \times p_{mean} \quad (5)$$

Thus a plot of the relative permeance against the mean pressure offers an easy tool to determine the average pore sizes of different membranes, by direct comparison of the curve slopes.

Asymmetric membranes can be treated in a similar way as a number of different resistances in series, for each of which the flow must be described by an equation such as eq. (1). The final result is a nonlinear equation describing the permeance in terms of the individual "layers":

$$(P / L)_{overall} = [\sum(P / L)_i^{-1}]^{-1} = [\sum(A_i + B_i \times p_{mean,i})^{-1}]^{-1} \quad (6)$$

As $p_{mean,i}$ of each "layer" is unknown and dependent on $(P/L)_{overall}$, this nonlinear equation can only be solved iteratively.[28] It describes a convex curve in which the curvature is in some way a measure of the asymmetry of the membrane. In a similar way as for eqs. (1) and (5), the relative permeance can be calculated using the intercept value with the y-axis, obtained from an iterative fit of the experimental data with eq. (6). For simplicity, and as a first approximation, for the present analysis we will use a standard least squares fit with a 2nd or 4th order polynomial instead of eq. (6) to obtain the intercept value $(\Sigma A_i^{-1})^{-1}$ from the plots of the permeance versus mean pressure.

Summarizing the above we can conclude that, while the absolute permeance describes the overall transport properties, the pressure dependence of the relative permeance is a measure of the average effective pore size and the deviation from linearity gives information on the asymmetry of the membrane.

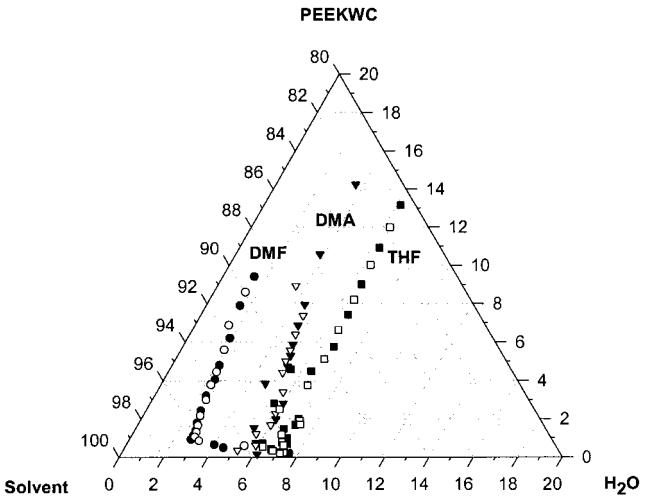

Figure 1 Phase diagrams of the ternary systems PEEKWC/DMF/water, PEEKWC/DMA/water, and PEEKWC/THF/water and PEEKWC/DMF/isopropanol determined by visual cloud point observation at room temperature. Closed symbols represent the clear-turbid transition upon nonsolvent addition; open symbols represent the turbid-clear transition upon solvent addition. The arrow gives a qualitative sketch of the concentration path during the demixing process.

EXPERIMENTAL

Materials

PEEKWC was supplied by the Chanchung Institute of Applied Chemistry, Academia Sinica. The polymer powder was purified by Soxhlet extraction with methanol and dried in a vacuum oven. *N*,*N*′-dimethylformamide (DMF), *N*,*N*-dimethylacetamide (DMA), THF, and isopropanol were purchased from Fluka and used without further purification. Water, used for the coagulation bath, was double distilled.

Phase diagrams

Phase diagrams, at room temperature (~ 20°C), were determined by visual observation of the cloud point during slow addition of the nonsolvent to the stirred polymer solution. After the cloud point was reached, an extra amount of nonsolvent was added and then the opposite procedure was followed: determination of the point where the solution became clear again by slow addition of solvent ("clearing point"). The procedure was repeated several times until the system became too dilute to observe turbidity changes accurately.

Membrane preparation and characterization

The purified polymer was dissolved at room temperature in the solvents DMA, DMF, and THF at three different concentrations (10, 15, and 19 wt %). The solution was magnetically stirred for at least 1 day to guarantee complete dissolution of the polymer. The casting solu-

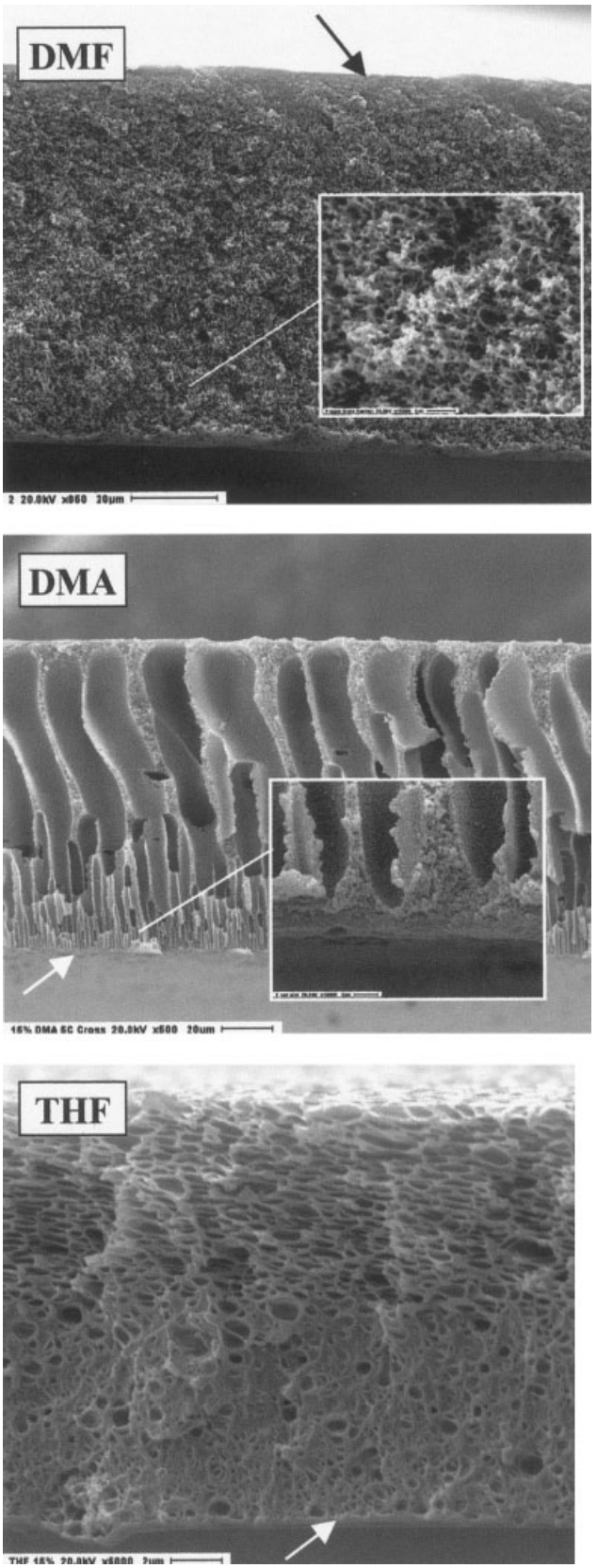

Figure 2 SEM pictures of the membranes prepared from a 15 wt % PEEKWC solution in DMF, DMA, and THF, coagulated in water (at higher magnification, detail of the skin layer). Arrow indicates the skin layer.

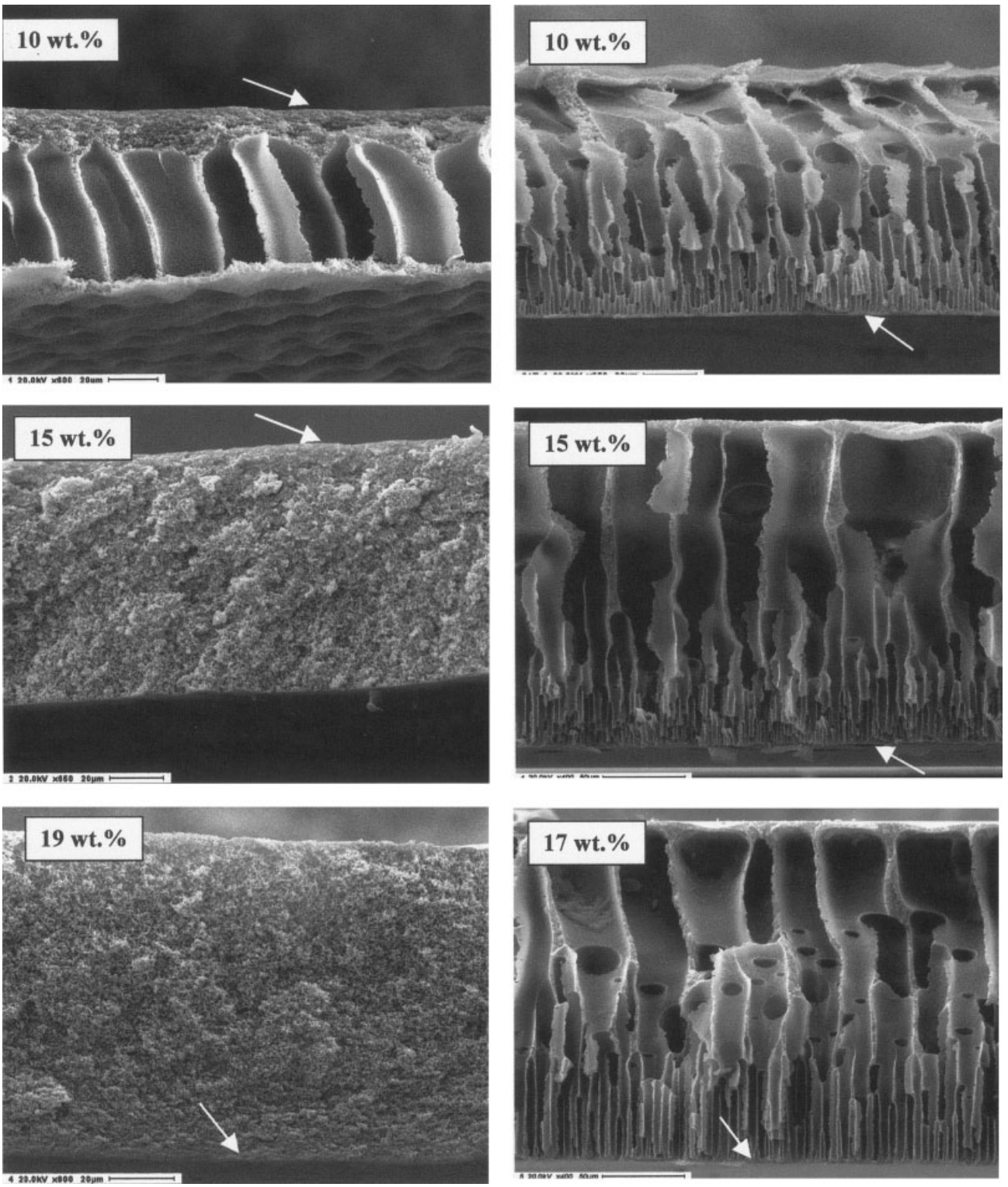

Figure 3 SEM images of the cross-sections of membranes prepared from PEEKWC solutions in DMF (left) and DMA (right) at different polymer concentrations. Coagulation in water at 25°C; interval between casting and coagulation 45 s. Arrow indicates the skin layer.

tions were centrifuged to remove macroscopic impurities present in the PEEKWC powder. The solutions were cast uniformly onto a glass substrate by means of a hand-casting knife (BRAIVE Instruments) with a knife gap set at 250 μm and then immersed in a coagulation bath after exposure for a fixed time to the air. An overview of the experimental conditions is reported in Table II. After complete coagulation, the membranes were

transferred into a pure water bath, which was refreshed frequently for at least 24 h to remove the traces of solvent. The membranes were stored in a deionized water bath until tested for water permeability; for gas permeance measurements the membrane samples were dried at 60°C under vacuum.

The morphology of the dried membranes (at 60°C overnight) was examined using scanning electron microscopy (SEM: Cambridge, Stereoscan 360) at 20 kV. For cross-section analysis the membrane samples were freeze fractured in liquid nitrogen. All samples were sputter-coated with gold before analysis.

Ultrafiltration water flux measurements were carried out using an ultrafiltration setup (Separem Type UFSCP) consisting of five parallel filtration cells, each one offering an effective filtration area of 19.2 cm^2. Transmembrane pressures (ΔP) were varied from 1 to 4 bar and the temperature was fixed at 25°C.

The membrane thickness was determined by a digital micrometer (Carl Mahr D 7300 Esslingen a.N.) and by SEM observation of the freeze-fractured cross-sections. The overall porosity, ϵ, of the membranes was calculated according to the equation:

$$\varepsilon = 100\% \times (1 - \text{density}_{\text{membrane}} / \text{density}_{\text{PEEKWC}}) \quad (7)$$

in which the density of the membrane was determined gravimetrically by weighing a sample of known area and thickness.

The pure gas permeance of the membranes was measured on a testing instrument constructed by GKSS Forschung, Germany. The instrument consists of a thermostated membrane cell with fixed permeate volume at the feed side connected via a series of control valves to different gas flasks. The procedure is based on a pressure increase measurement on the fixed volume permeate side of the membrane cell, which is completely evacuated before the start of the measurement. For characterization of porous membranes, measurements were carried out at 25°C at a series of nitrogen gas pressures ranging from about 100 to 1,200 mbar. For permselective membranes, measurements were carried out with five different gases (nitrogen, oxygen, methane, helium, and carbon dioxide) at ~ 1 bar. The membranes prepared from 15 and 19 wt % solutions in THF were found to have a dense selective layer and were measured at a single feed pressure with different gases to determine the permselectivity.

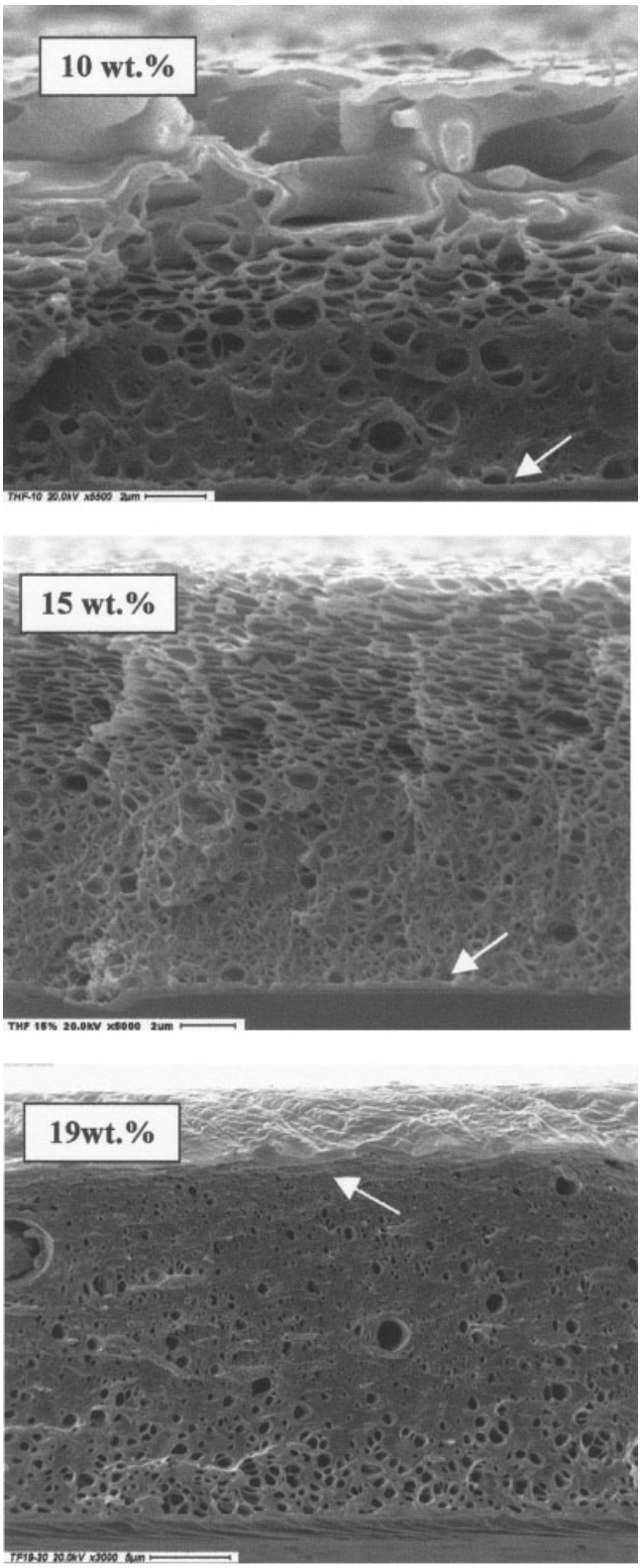

Figure 4 Cross-sections of membranes prepared at different concentrations of PEEKWC in THF using water as coagulant. Coagulation at 25°C; interval between casting and coagulation 20 s. Arrow indicates the skin layer.

RESULTS AND DISCUSSION

Phase diagrams

The ternary phase diagrams of the three PEEKWC/solvent/water systems were determined by cloud point measurements. The results are shown in Figure 1. We can see that the amount of water needed to induce phase separation decreases in the order THF > DMA > DMF, thus with increasing polarity of the

TABLE III
Influence of the Concentration of the Casting Solution on the Membrane Thickness and the Overall Porosity[a]

Solvent	DMA			DMF		
Concentration (wt %)	10	15	17	10	15	19
Thickness[b] (μm)	95 (106)	199 (200)	211 (212)	71 (70)	96 (90)	99 (120)
Overall porosity[c] (%)	87	85	79	79	77	70

[a] Casting and coagulation temperature 25°C; interval between casting and coagulation 45 s.
[b] Thickness from SEM image; values in parentheses were measured with a micrometer, average value of at least 3 points.
[c] Porosity calculated on the basis of the thickness measured with a micrometer.

solvent. Such a shift of the binodal demixing curve to higher nonsolvent concentrations is often related to a reduced solvent/nonsolvent interaction and typically leads to delayed demixing.[15,30] In fact, also during membrane preparation, clear differences are observed in the coagulation behavior of the three systems. Upon immersion in the coagulation bath, the solutions in DMA and DMF turn white immediately, indicating an instantaneous demixing. With the THF solution, only after some time the cast film becomes opaque, first only slightly and then gradually more so until it also becomes completely white. The described behavior can easily be understood from the qualitative sketch of the concentration paths, drawn in the phase diagrams. These confirm the increased tendency toward delayed demixing with increased width of the miscibility gap.

The width of the miscibility gap is a very important parameter in relation to the type of demixing process and therefore the proper choice of the solvent/nonsolvent combination is of fundamental importance the morphology development, as will be shown later in this paper.

For higher polymer concentrations, extrapolation of the binodal demixing curve is necessary, as the viscosity of the solution, above $\sim$ 15 wt %, becomes too high for efficient stirring and reproducible determination of the cloud point. In practice, the starting concentration during the film formation is often higher, in particular in the case of THF, where significant evaporation of the solvent may occur in the time interval between film casting and coagulation. It is important to note that no difference is observed between the cloud points and the "clearing" points, confirming the validity of the experimental procedure. Some scatter in the low concentration range is due to the increasingly difficult visual observation of changes in turbidity at high dilutions.

Influence of the casting solution

Solvent type

The SEM analysis shows a strong difference in the membrane morphology by changing the type of solvent in the casting solution, using water as the nonsolvent in the coagulation bath. Figure 2 shows that the morphology of membranes prepared from a 15 wt % polymer solution varies from porous sponge-like for DMF and porous finger-like for DMA to a highly asymmetric structure with a dense skin layer for THF.

In particular, the membrane prepared with DMF presents an interconnected pore structure from skin to sublayer. At very high magnification ($\times$35,000) a large number of small pores is observed on the top surface. The maximum pore dimensions are about 100–200 nm.

In the case of DMA the skin region of the membrane consists of a thin top layer with a typical structure of closely packed polymeric spheres, a so-called nodular structure, supported by elongated macrovoids. SEM observation shows a smooth surface. The phase diagram of the PEEKWC/DMA/water system suggests that the critical point lies at a very low polymer concentration, and hence that the metastable region is always entered above the critical point (Fig. 1). According to the literature, this should lead to nucleation from the polymer lean phase, which is incompatible with the observed nodular structure.[8] A possible explanation for the formation of such structure could be that spinodal demixing occurs.[9,10]

Based on the phase diagrams, the demixing should be more instantaneous in the case of DMF than in the case of DMA. Instantaneous demixing is often closely related to the formation of macrovoids. The fact that with the present systems the tendency to form macrovoids is much stronger in the case of DMA than in the case of DMF is a clear indication that, besides thermodynamics, kinetic factors also play an important role in the morphology development.

In the case of DMF, the adsorption of atmospheric humidity is more rapid with respect to DMA, which promotes a more homogeneous pore nucleation compared to its growth. Below, the effect of the air exposure time before immersion confirms this hypothesis.

Using THF as the solvent, a highly asymmetric membrane is obtained; a porous sublayer with a closed cell structure, in which the size, as well as the number of the cells, gradually decreases, moving from the bottom toward the completely dense skin layer. This is mainly due to the high volatility of THF, which causes an increase of the polymer concentration at the interface: the low THF/Water miscibility determines the formation of closed cells.

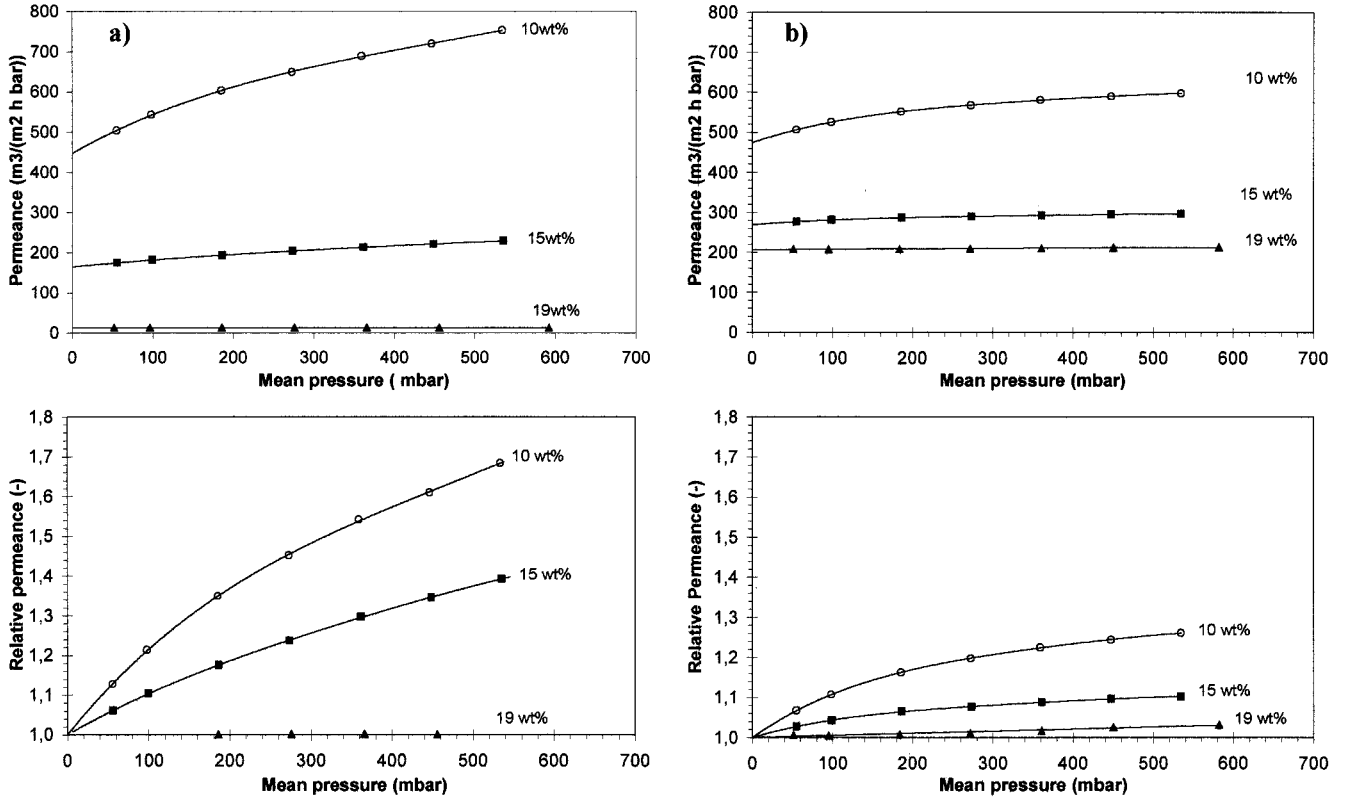

Figure 5 Absolute (top) and relative permeance (bottom) of membranes prepared at different casting solution concentrations (10, 15, and 19 wt %) with (a) DMA/PEEKWC/water system and (b) DMF/PEEKWC/water system as a function of the mean pressure difference across the membrane.

Polymer concentration

Figures 3 and 4 show the effect of PEEKWC concentration on membrane morphology (cross-sections) for the membranes prepared with different solvents. The influence of the polymer concentration in the casting solution on the morphology is relatively small for the

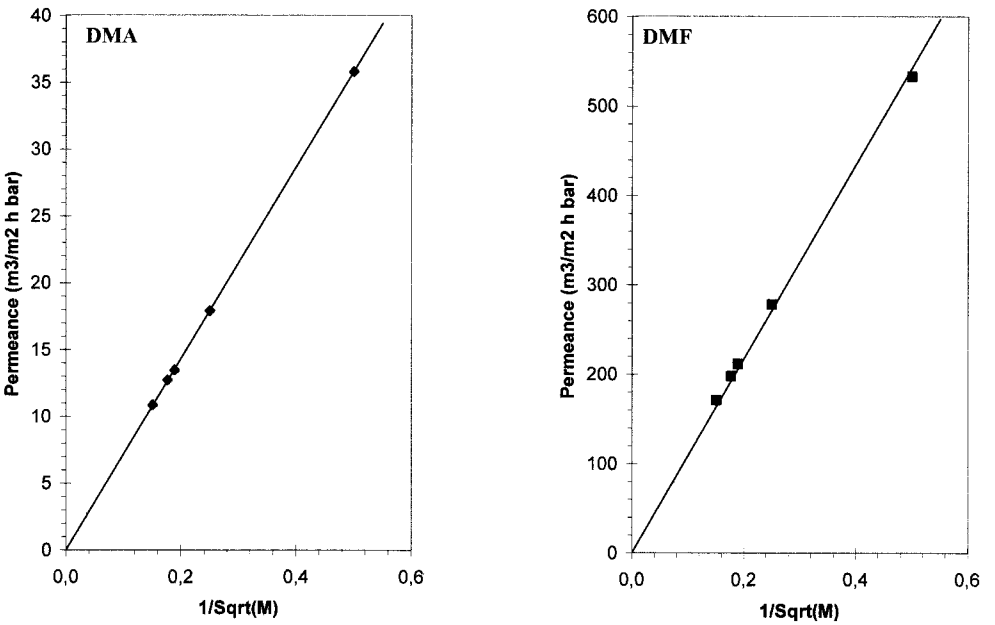

Figure 6 Plot of the permeance against (molar mass of the permeating gas)$^{-0.5}$ for the membranes prepared from 19 wt % solutions in DMA and DMF.

TABLE IV
Gas Permeability and Permselectivity of the Membranes Prepared from THF at Polymer Concentrations of 15 and 19 wt %

Gas	15% PEEKWC in THF		19% PEEKWC in THF		Pure dense PEEKWC [33]	
	Permeance (10^{-5} m^3/m^2 h bar)	Selectivity (−)	Permeance (10^{-5} m^3/m^2 h bar)	Selectivity (−)	Permeance (10^{-5} m^3/m^2 h bar)	Selectivity (−)
Helium	161	56	93	49	152	71.6
CO_2	71	25	47	25	68.3	32.3
Oxygen	14	4.8	84	4.4	12.5	5.9
Methane	3.1	1.1	2.8	1.5	1.87	0.88
Nitrogen	2.9	1.0	1.9	1.0	2.12	1
Thickness[a] (μm)	20 (19)		25 (25)		15	
Effective thickness[b] (μm)	14.2		24.5			

[a] Thickness from SEM; values in parentheses are the average of at least 3 points determined with a micrometer.
[b] From comparison of helium flux of dense and asymmetric membrane.

membranes prepared from DMA, where the morphology is dominated by large macrovoids. The main effect is an increase of the membrane thickness and a slight decrease of the overall porosity with increasing polymer concentration (Table III). The latter is also observed in the case of DMF. In addition, in the case of DMF, it is clear that a higher polymer concentration can suppress the formation of finger-like voids.

The strongest effect is observed in the case of THF, where an increase of the polymer concentration in the casting solution leads to nearly complete disappearance of the pores and the formation of an almost dense membrane. The influence of the polymer concentration is best observed in relation with the transport properties of the membranes (see below).

Transport properties

Gas permeability measurements were used for a first qualitative evaluation of the membrane transport properties. In the present work the nitrogen permeability of all membranes at feed pressures ranging from ~ 100 to 1,200 mbar has been measured. Only the membranes prepared from a THF solution were dense and were tested at a single pressure with different gases to determine their permselectivity. This procedure was also used for porous membranes with very low permeability to check for the applicability of the Knudsen diffusion model.

Data analysis in the present work was slightly simplified in the sense that we have fitted the pressure

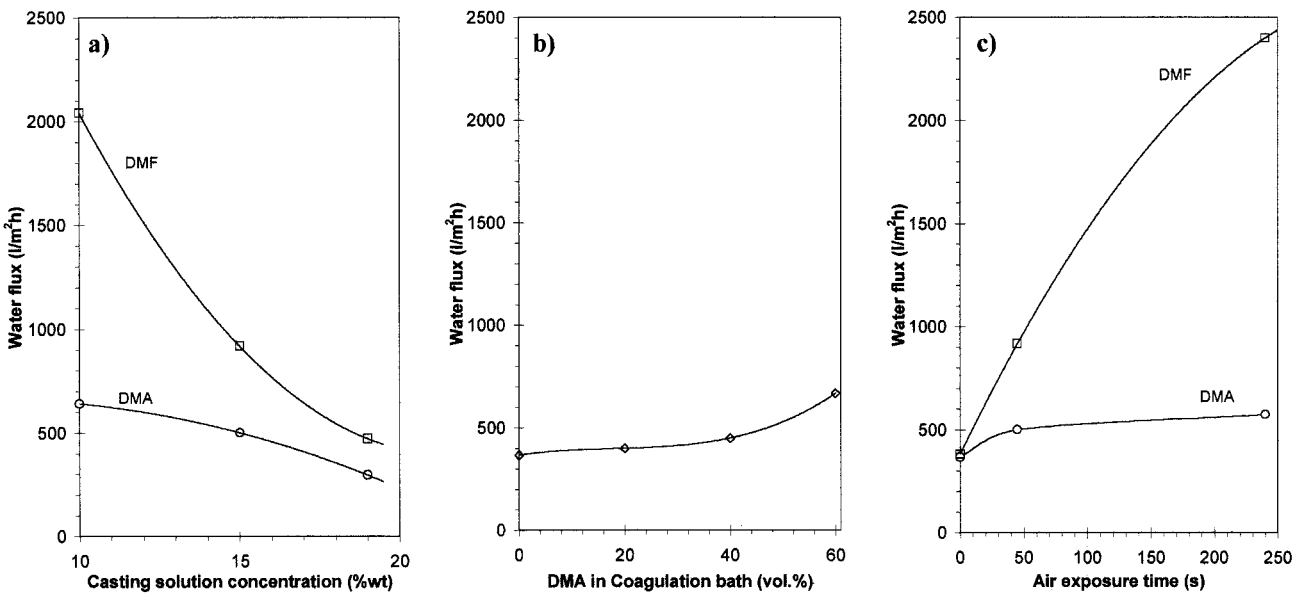

Figure 7 Water flux of membranes prepared from PEEKWC solutions (a) in DMA and DMF at different polymer concentrations; (b) in DMA and coagulated in a water coagulation bath containing 0, 40, and 60 vol % of DMA; and (c) in DMA and DMF with increasing intervals between film casting and coagulation.

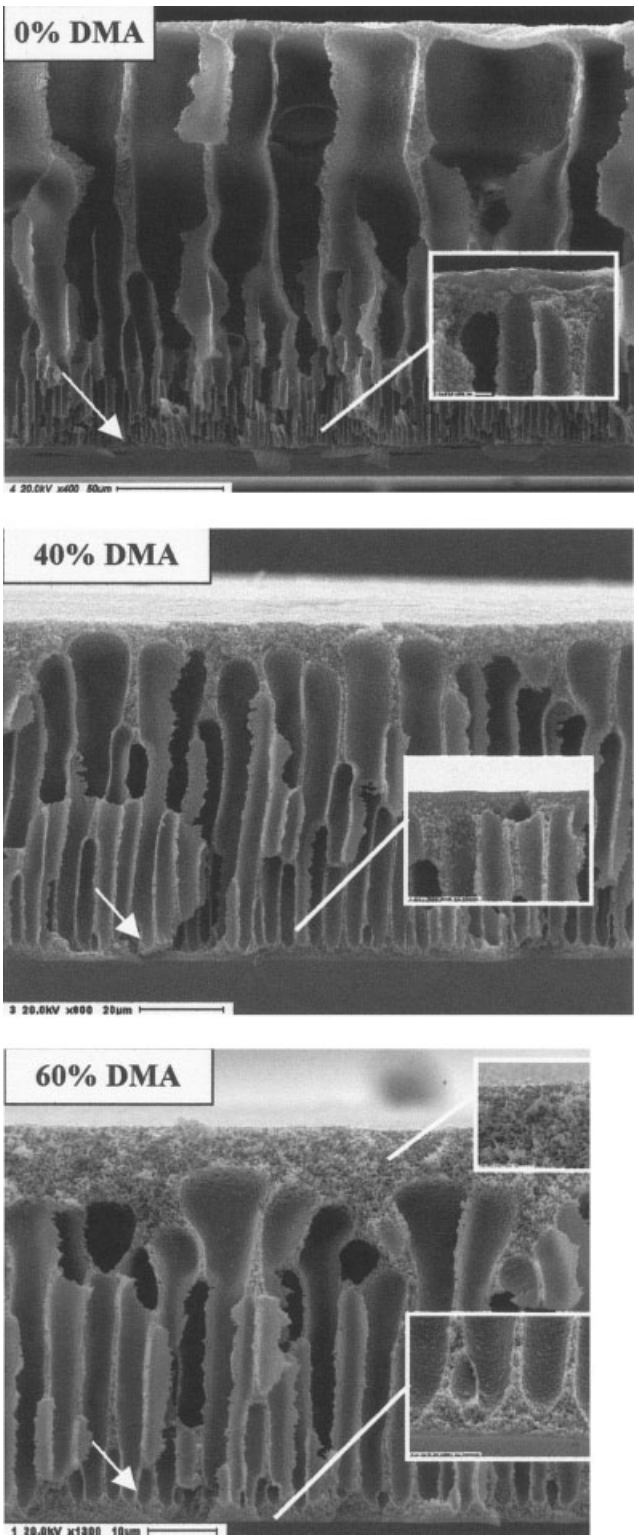

Figure 8 Morphologies of the membranes prepared from a 15 wt % solution in DMA and coagulated in a water bath containing different amounts of DMA. Coagulation temperature 25°C; interval between casting and coagulation 0 s. Insets: detail of the skin and/or bottom layer. Arrow indicates the skin layer.

dependence of the permeance with a standard least squares fit with a 2nd or 4th order polynomial, rather than solving eq. (6) iteratively to obtain the intercept value $(\Sigma A_i^{-1})^{-1}$. The main results are displayed in Figure 5.

For both solvents the permeance strongly decreases with increasing polymer concentration in the casting solution. This effect is most evident for DMA, where the flux decreases by more than two orders of magnitude. At the same time the relative permeance decreases with increasing polymer concentration, which indicates a decrease of the average pore size [eq. (4)[rsqb]. Also here the effect is strongest for DMA. The difference between the two systems with DMA and DMF can be related to their microstructure. It was shown that DMF gives a sponge-like porous structure. With increasing polymer concentration the membrane thickness clearly increases while the overall porosity tends to diminish (Table III), resulting in both lower fluxes and smaller pores. With DMA, however, the membranes show large macrovoids and the transport properties are mainly determined by the relatively thin top layer. At 19 wt % of polymer the flux collapses drastically and the permeance becomes practically pressure-independent, as can be seen from the plot of the relative permeance. This behavior is compatible with either the solution-diffusion mechanism or with Knudsen diffusion. From the linear relationship between the permeance and the reciprocal square root of the molar mass[32] in Figure 6, it follows that Knudsen diffusion occurs and that the membrane has a nanoporous skin layer. For the membrane prepared from a 19 wt % solution in DMF, a slight deviation from this linear relationship is due to the higher pore size and the combination of Knudsen and Poiseuille flow.

Gas permeation measurements on the membranes prepared from THF confirm what was already suggested by the SEM observations. These membranes exhibit a high permselectivity for different gases (see Table IV), which means that they have a dense skin layer. The permselectivity is slightly lower than that of dense membranes prepared from a chloroform solution by solvent evaporation,[33] probably due to pinholes. This is a common problem in asymmetric membranes prepared by phase inversion techniques and it can easily be solved by applying a coating on the selective layer.[34] The "faster" gases, such as helium, are relatively insensitive to these defects. Confrontation of the helium permeability of the asymmetric membranes and a 15-μm dense membrane allows for the calculation of the effective thickness of the active layer of the asymmetric membranes. These values are also reported in Table IV. For the present membranes these values are rather high and further optimization of the procedure is required to obtain an open interconnected porous sublayer with a thin defect-free skin layer. This objective may be reached by carefully balancing two variables: the time interval between casting and coagulation and the nonsolvent concentration in the casting (work in progress). Only at the lowest

TABLE V
Influence of the Coagulation Bath Composition for the System DMA/PEEKWC/Water and DMF/PEEKWC/Isopropanol on the Membrane Thickness and Overall Porosity

System	DMA/PEEKWC/Water			DMF/PEEKWC/Isopropanol		
Coagulation bath composition (vol % solvent)	0	40	60	0	25	50
Thickness (μm)[a]	200	80	62	56 (87)	53 (42)	40 (32)
Overall porosity (%)	74	70	68	65	60	52

[a] Thickness determined with SEM; values in parentheses were determined with a micrometer (average value of 3 points).

polymer concentration in the casting solution (10%) does the membrane become porous, with few relatively large pores.

The water fluxes strongly decrease with increasing polymer concentration in the casting solution (Fig. 7). For all concentrations the membranes from DMF have a higher permeance than those prepared from DMA. In general, the water flux shows the same trend as the gas permeation measurements with the 19 wt % solution in DMA, which has a relatively high water flux, being the only exception. This may be due to the differences in membrane treatment (see Experimental). For the water permeation measurements the membranes were always conserved in water prior to the measurement, whereas the membranes for the gas permeation were dried at 60°C. This may have caused a final densification of the porous structure, leading to low gas fluxes.

Influence of the coagulation bath

Solvent/nonsolvent mixtures

DMA-H_2O. As shown above, all membranes prepared from DMA solutions have a finger-like void structure. For practical application of the membranes, this is undesired as it reduces their mechanical stability.[34] Macrovoid formation is usually a result of a fast demixing during the phase inversion process[8,11] and a possible solution to this problem is therefore the addition of solvent to the coagulation bath. It is generally known that, when solvent and nonsolvent have a strong interaction, the addition of solvent to the coagulation bath promotes the formation of a sponge-like rather than a finger-like morphology.[12] Therefore, two experiments in which DMA was added to the coagulation bath, 40 and 60 vol %, respectively, have been carried out. Unfortunately, Figure 8 shows that the formation of macrovoids could not be completely suppressed, although their shape becomes less elongated and both the skin and the bottom layer become more spongy. A remarkable side effect is that the total membrane thickness drastically decreases with the addition of DMA to the water bath (Table V) and as a consequence the overall porosity also decreases. This is due to the slower demixing and the slower gelation of the polymer rich phase, which allows a stronger contraction of the polymeric film in a perpendicular direction.

DMF-isopropanol. As reported above, DMF gives the desired sponge-like membrane and, by changing the polymer concentration in the casting solution, the pore size is influenced. However, the obtained pore sizes are still high for ultrafiltration applications. In general, the pore size can be reduced by the use of nonsolvents with a lower affinity toward the solvent.[11,35] Therefore, isopropanol as coagulant has been used. To slow down the demixing process even further, addition of DMF to the isopropanol coagulation bath has been carried out.

SEM images show that the membranes, coagulated in isopropanol, have large internal cavities between a sponge-like top and bottom layer, which become even larger with increasing DMF content in the coagulation bath (Fig. 9). Apparently the effect of the more dense skin, which may induce macrovoids,[13] dominates that of the slower demixing, which usually suppresses macrovoid formation. At higher DMF concentration in the coagulation bath, the sponge-like character of the top and bottom layer disappears and the skin demonstrates clear pinhole defects. Probably part of the differences, compared with the DMF/water system, may simply be ascribed to the larger dimension of the isopropanol molecule and thus to the slower diffusion through the top layer of the nascent membrane. To obtain homogeneously porous membranes, the pore nucleation must be much faster than pore growth and, in addition, nucleation must occur throughout the entire thickness of the cast film. The latter requires fast diffusion of the nonsolvent deeply into the film, which may be problematic in the case of larger nonsolvent molecules like isopropanol.

As observed earlier for the DMA/water system and the DMF/isopropanol system, the addition of solvent to the coagulation bath leads to a reduction of the overall membrane thickness and overall porosity (Table V). This is a consequence of the slower phase separation and, in particular, of the slower solidification of the nascent membrane. The latter leaves more time for the dissolved or swollen polymeric chains to contract themselves in the increasingly unfavorable solubility conditions, before the structure is definitively fixed by gelation.

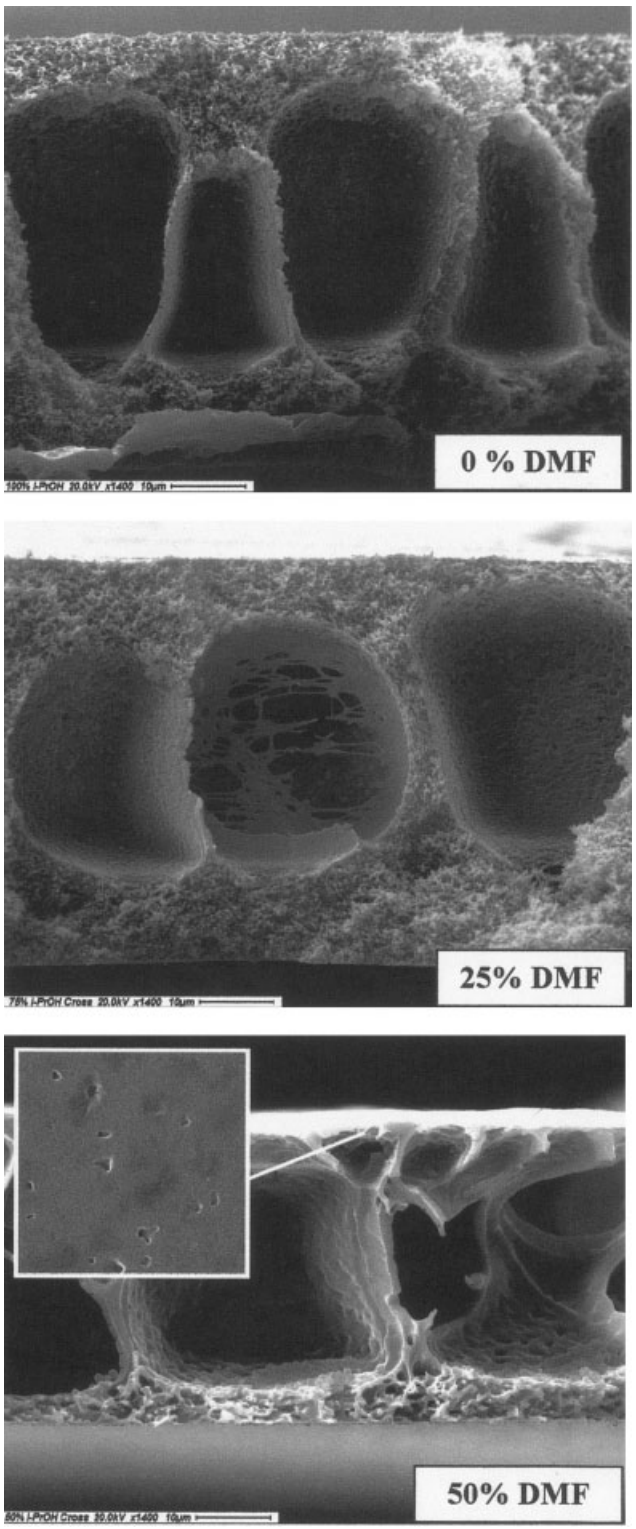

Figure 9 Cross-sections of the membranes prepared from a 15 wt % solution in DMF and coagulated in isopropanol with different amounts of DMF. Coagulation temperature 25°C; interval between casting and coagulation 0 s. Inset: detail of the skin layer.

Transport properties

DMA/H_2O. In Figure 10 the absolute and relative permeance of membranes prepared by using different coagulation bath compositions is shown. The gas permeability shows a strong increase at higher DMA content in the coagulation bath. This is in perfect agreement with the observed change in morphology from finger-like with a (nearly) dense skin to increasingly spongy (Fig. 8). The highest nitrogen permeance is observed with the membrane prepared by using 60 vol % DMA in the coagulation bath and is about two orders of magnitude higher than the membranes prepared using pure isopropanol in the coagulation bath. In contrast, the slopes of the relative permeance curves do not reveal an unambiguous influence of the coagulation bath composition on the average pore diameter. The membrane prepared with pure water as the coagulant surprisingly shows the highest average pore size, despite its very low permeability. This may be an indication of the presence of defects in the skin layer.

The trend in the water fluxes (Fig. 7) is the same as that of the gas permeability, i.e., increased permeability with increasing DMA concentration in the coagulation bath, but the absolute differences in permeability are much smaller. This might be related to the drying of the membranes prior to the gas permeation tests, which probably induces a minor contraction of the skin layer and a reduction of the pore size.

DMF/isopropanol. Comparison of the membranes coagulated in water and in isopropanol (Fig. 11) shows that the latter indeed have a somewhat lower gas permeability, in agreement with the expected slower demixing process, resulting in a less porous top layer.[13,36] However, for reasons not yet fully understood, with isopropanol the average pore size is larger and the active layer is more symmetric, as can be seen from the linear pressure dependence of the relative permeance. A more significant reduction of the permeability and the average pore size is achieved by addition of DMF to the coagulation bath. Addition of very large amounts of DMF to the coagulation bath, however, leads to the formation of pinhole defects ($\sim$ 0.5 μm, Fig. 9) in the top layer with a consequent increase of the permeability.

As reported in the literature,[8] the addition of the solvent to the coagulation bath induces delayed demixing of the cast film due to a decrease of the overall mass transfer rate. However, an increasing solvent concentration in the coagulation bath leads to a decrease in the polymer concentration at the interface. Therefore, two phenomena, which have an opposite effect on the membrane morphology, occur: delayed demixing tends to produce membranes with a lower porosity, whereas low interfacial polymer concentration tends to produce a more open top layer.

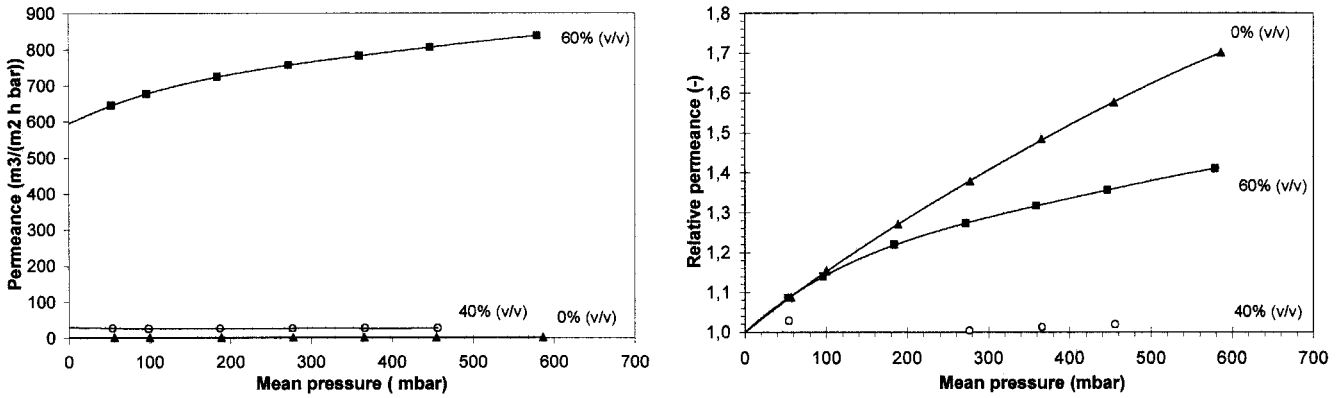

Figure 10 Absolute and relative permeance of membranes prepared from a 15 wt % solution in DMA, coagulated in a water bath with different amounts of DMA. Coagulation at 25°C; interval between casting and coagulation 0 s.

Influence of the exposure time before bath immersion

Morphology

Figure 12 shows the SEM images of the membranes prepared from casting solutions in DMA and in DMF, varying the exposition of the cast films to the air, prior to the immersion into the coagulation bath. In both cases the effect is the same: without exposure to the air a membrane with a finger-like macrovoid structure is obtained; on exposure to the air the membranes become sponge-like with a very fine interconnected pore structure, which becomes larger upon further exposure. Another effect of prolonged exposure to the air is the formation of micrometer size pores in the membrane surface. The observed change in morphology is due to changes of the kinetics of the phase separation process:[37–39] absorption of humidity from the air by

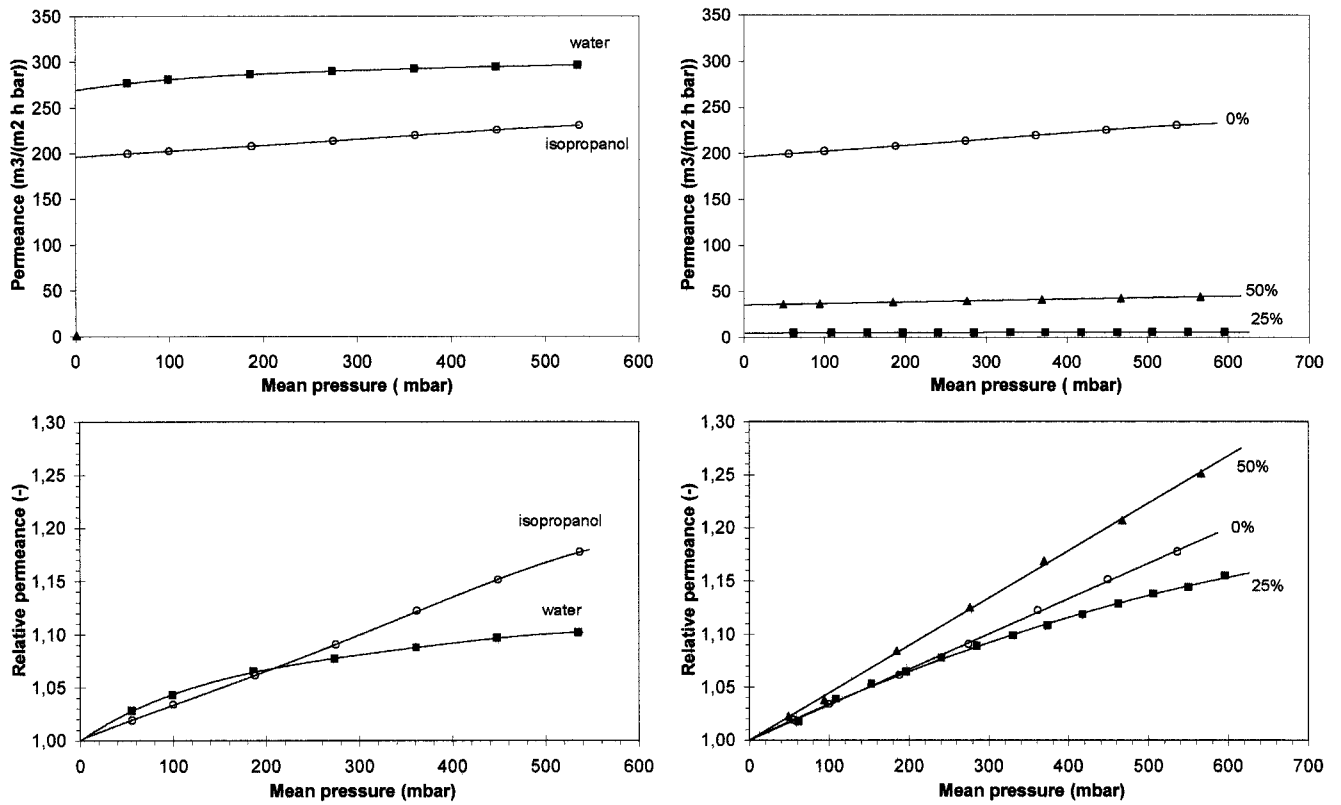

Figure 11 Absolute (top) and relative permeance (bottom) of membranes prepared from a 15 wt % solution in DMF. Coagulation in water and in isopropanol (left) and coagulation in isopropanol with different amounts of DMF (right). Coagulation temperature 25°C; interval between casting and coagulation 0 s.

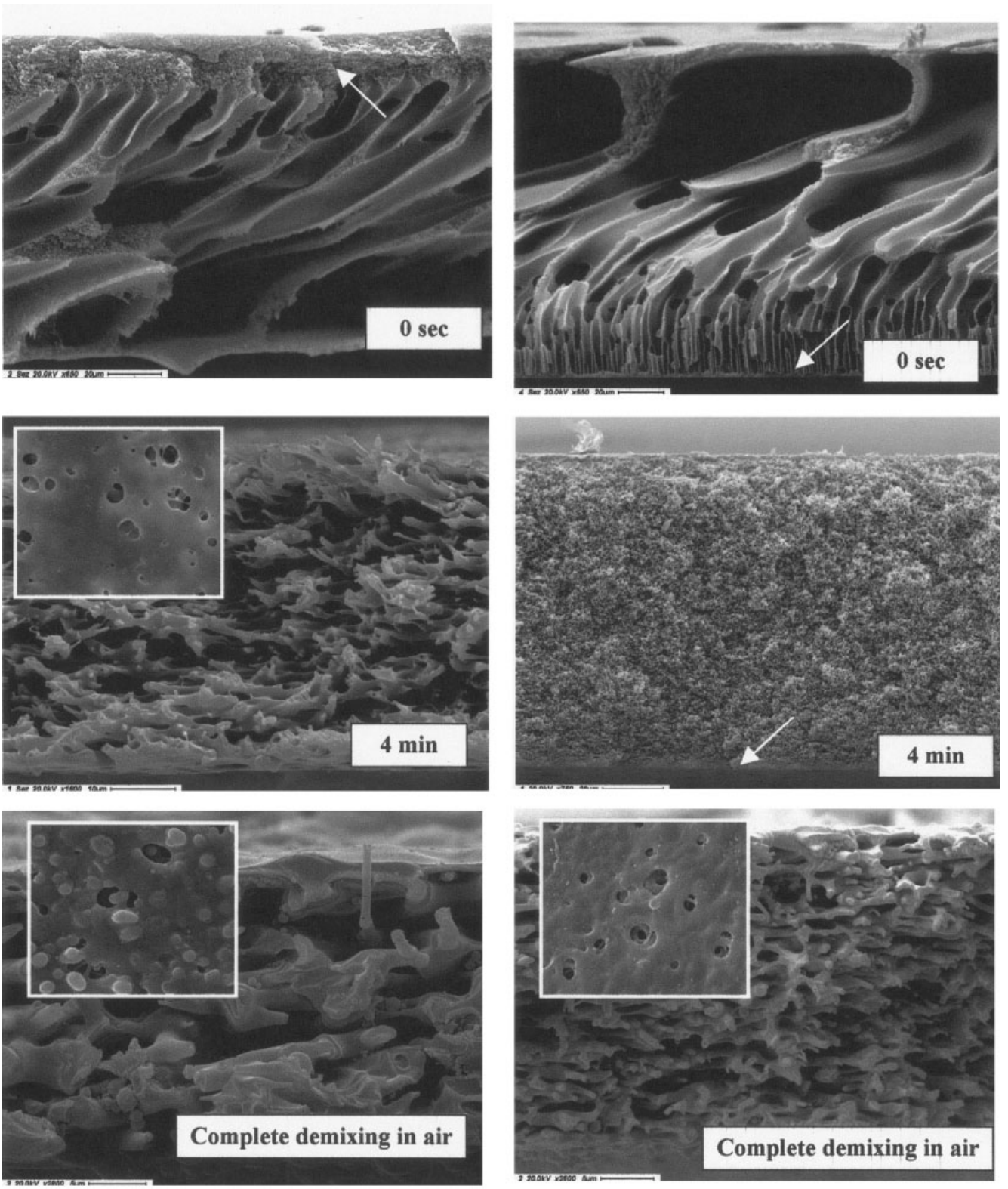

Figure 12 Cross-sections of the membranes from a 15 wt % PEEKWC solution in DMF (left) and DMA(right) prepared by varying the exposure time before immersion in the water coagulation bath (at higher magnification, detail of the surface, skin layer). Arrow indicates the skin layer.

the hygroscopic solvents used brings the cast film closer to demixing conditions. It reduces the gradient of the water concentration in the nascent membrane film upon contact with the coagulation bath and thus promotes more homogeneous nucleation. In the extreme case of very long exposure times, the demixing

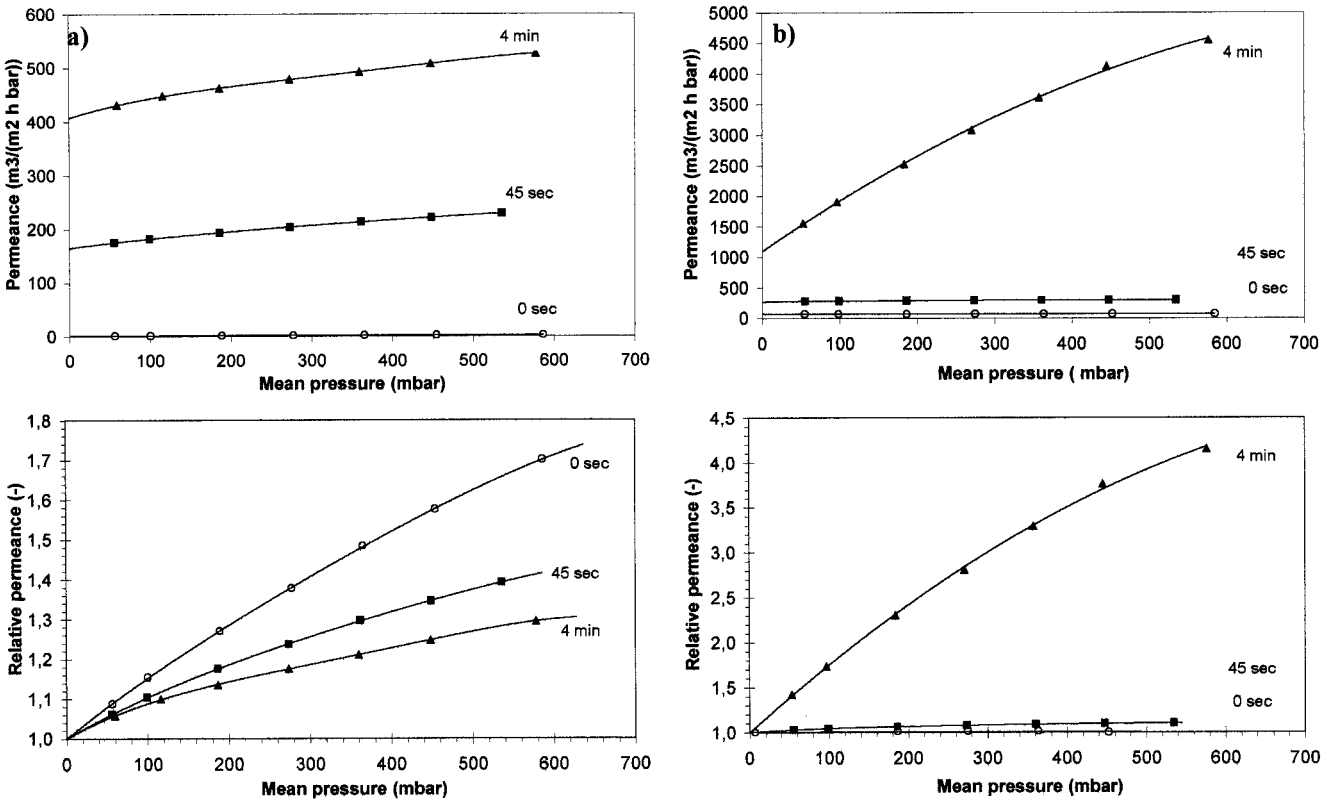

Figure 13 Absolute and relative permeance of membranes prepared with different time intervals between casting and coagulation. Casting solution in DMA (a) and DMF (b). Coagulation in water at 25°C.

already begins before immersion into the coagulation bath. This is accompanied by a reduction of the membrane thickness, due to slow simultaneous evaporation of the solvent.

All of these phenomena are more rapid in the case of DMF than in the case of DMA, which is in agreement with the phase diagrams (Fig. 1), showing that the binodal demixing curve in DMF lies at lower water concentrations than that in DMA. It is worth noting that, with the DMA solutions under the given experimental conditions, the formation of macrovoids could only be avoided by controlling the time interval between casting and coagulation. Neither by increasing the polymer concentration in the casting solution nor by adding solvent to the coagulation bath could complete suppression of macrovoids be achieved.

The suppression of macrovoids was probably a result of more rapid nucleation of pores: the cast film exposed to the air slowly absorbs humidity and the solution approaches the binodal demixing conditions. Subsequent immersion into the water coagulation bath then unleashes a rapid nucleation throughout the entire thickness of the cast film, in contrast to the unexposed film, where nucleation and pore growth take place from the surface inward. The result is a sponge-like morphology in the former and a macrovoid structure in the latter.

Transport properties

For both systems the nitrogen permeance of the membranes increases significantly upon exposure of the cast film to the air (Fig. 13), which is in agreement with the more open sponge-like pore structures obtained. Comparing the absolute and relative permeances for the two systems, it can be concluded that DMF gives relatively high fluxes and small pores, with the only exception being the membrane exposed for 4 min to the air, which has excessively large pores. With DMF the effective average pore size increases with increasing exposure of the cast film to the air. The very low flux of the membrane prepared with DMA without exposure to the air is probably due to the formation of a (nearly) dense skin, in which pinhole defects are responsible for the relatively high apparent pore size.

Water flux measurements are in good agreement with the observed gas permeabilities (Fig. 7). For both solvents the water flux increases with the exposure time of the cast film to the air. This effect is the strongest for DMF, which, in addition, gives the highest absolute fluxes.

CONCLUSION

Asymmetric PEEKWC membranes, with a wide range of different morphologies and transport characteris-

tics, can be produced by the wet phase inversion method. Membranes range from porous microfiltration and ultrafiltration membranes to dense gas separation membranes. Further optimization of the membrane preparation conditions for each specific application is necessary and will be subject of future work.

The position of the binodal demixing curve in a ternary phase diagram cannot completely describe the formation mechanism of PEEKWC membranes. Other factors, such as the affinity between the solvent and nonsolvent, the polymer concentration in the casting solution, and the interval between film casting and coagulation, have to be considered.

The nature of the solvent is fundamental for the type of morphology to be obtained: DMA and DMF give porous asymmetric membranes, the former usually with a (nearly) dense skin and a finger-like pore structure, the latter predominantly sponge-like; THF gives asymmetric membranes with a dense permselective top layer, suitable for gas separation.

Exposure of the cast film to the air also has a marked influence on the morphology and, in the case of DMF and DMA as the solvents, allows the suppression of macrovoids and the dense skin, resulting in higher permeabilities.

A higher polymer concentration in the casting solution has little effect on the overall morphology but results in membranes with a more dense skin layer with smaller pores, exhibiting a lower permeability.

The use of "softer" coagulation conditions has a different effect depending on the specific system, DMA/PEEKWC/water or DMF/PEEKWC/isopropanol. For DMA solutions the addition of DMA to the water coagulation bath increases the permeability and the sponge-like character of the membrane but it cannot avoid completely the formation of macrovoids. In the case of DMF solutions the use of isopropanol instead of water and the addition of DMF to the isopropanol coagulation bath reduces the permeabilty and promotes the formation of macrovoids.

References

1. Zhang, H. C.; Chen, T. L.; Yuan, Y. G. Chin. Patent 1987; CN 85, 108, 751.
2. Liu, K. J.; Zhang, H. C.; Chen, T. L. Chin. Patent 1987; CN 85, 101, 721.
3. Drioli, E.; Zhang, H. C. Chimicaoggi 1989, 11, 59.
4. Golemme, G.; Drioli, E.; Lufrano, F.; Polym Sci 1994, 36, 1647.
5. Gordano, A.; Clarizia, G.; Torchia, A.; Trotta, F.; Drioli, E. Desalination 2002, 145, 47.
6. Buonomenna, M. G.; Figoli, A.; Jansen, J. C.; Davoli, M.; Drioli, E. In Membranes Preparation, Properties and Applications; Burganos, V. N.; Noble, R. D.; Asaeda, M.; Ayral, A.; LeRoux, J. D. Eds.; Proceedings of the MRS Boston Fall Meeting; Materials Research Society: Boston, MA, 2002; Vol. 752.
7. Tasselli, F.; Jansen, J. C.; Drioli, E. J Appl Polym Sci, to appear.
8. Mulder, M. Basic Principles of Membrane Technology; Kluwer: Dordrecht, The Netherlands, 1991.
9. Boom, R. M.; Wienk, I. M.; van den Boomgaard, T.; Smolders, C. A. J Membr Sci 1992, 73, 277.
10. Wienk, I. M.; Boom, R. M.; Beerlage, M.; Bulte, A.; Smolders, C. A.; Strathmann, H. J Membr Sci 1996, 113, 361.
11. Smolders, C. A.; Reuvers, A. J.; Boom, R. M.; Wienk, I. M. J Membr Sci 1992, 73, 259.
12. Kim, J.; Lee, K. J Membr Sci 1998, 138, 153.
13. Strathmann, H.; Kock, K.; Amar, P.; Baker, R. W. Desalination 1975, 16, 179.
14. Young, T-H.; Cheng, L-P.; Lin, D-J.; Fane, L.; Chuang, W-Y. Polymer 1999, 40, 5315.
15. Kim, J. H.; Min, B. R.; Won, J.; Park, H. C.; Kang, Y. S. J Membr Sci 2001, 187, 47.
16. Bulte, A. M. W.; Naafs, E. M.; van Eeten, F.; Mulder, M. H. V.; Smolders, C. A. Polymer 1996, 37, 1647.
17. Young, T. H.; Chen, L-W. Desalination 1995, 103, 233.
18. Cheng, L. P.; Young, T-H.; Chuang, W-Y.; Chen, L-Y.; Chen, L-W. Polymer 2001, 42, 443.
19. Barth, C.; Gonçalves, M. C.; Pires, A. T. N.; Roeder, J.; Wolf, B. A. J Membr Sci 2000, 169, 287.
20. Chun, K-Y.; Jang, S-H.; Kim, H-S.; Kim, Y-W.; Han, H-S.; Joe, Y-I. J Membr Sci 2000, 169, 197.
21. Reuvers, A. J.; Smolders, C. A. J Membr Sci 1987, 34, 67.
22. Reuvers, A. J.; van den Berg, J. W. A.; Smolders, C. A. J Membr Sci 1987, 34, 45.
23. Brandrup, J.; Immergut, E. H., Eds.; Polymer Handbook; John Wiley & Sons: New York, 1975; 2nd ed.
24. Johnson, M. B.; Wilkes, G. L. J Appl Polym Sci 2002, 84, 1076.
25. Buescher, U.; Gooding, C. H. J Membr Sci 1997, 132, 213.
26. Buescher, U.; Gooding, C. H. J Membr Sci 1999, 152, 99
27. Nakao, S. J Membr Sci 1994, 96, 131.
28. Meixner, D. L.; Dyer, P. N. J Membr Sci 1998, 140, 81.
29. Kong, J.; Li, K. J Appl Polym Sci 2001, 81, 1643.
30. Lonsdale, H. K. J Membr Sci 1982, 10, 81.
31. Kim, J. H.; Min, B. R.; Won, J.; Park, H. C.; Kang, Y. S. J Membr Sci 2001, 187, 47.
32. Baker, R. W. Membrane Technology and Applications; McGraw-Hill: New York, 2000.
33. Figoli, A.; Torchia, A.; Clarizia, G.; Drioli, E. Ital J Food Sci, to appear.
34. Peinemann, K. V.; Maggioni, J. F.; Nunes, S. P. Polymer 1998, 15, 3411.
35. Mckelvey, S. A.; Koros, W. J. J Membr Sci 1996, 112, 29.
36. Young, T. H.; Chen, L. W. J Membr Sci 1991, 57, 69.
37. Cheng, J. M.; Wang, D. M.; Lin, F. C.; Lai, J. Y. J Membr Sci 1996, 109, 93.
38. Altena, F. W.; Smolders, C. A. Macromolecules 1982, 15, 1491.
39. Pereira, C. C.; Nobrega, R.; Borges, C. P. J Membr Sci 2001, 192, 11.